

Report:
**Introduction of a Synthetic CO₂-Fixing
Photorespiratory Bypass into a
Cyanobacterium**

Patrick M. Shih, Jan Zarzycki, Krishna K.
Niyogi and Cheryl A. Kerfeld
J. Biol. Chem. published online February 20, 2014

METABOLISM

ENZYMOLGY

Access the most updated version of this article at doi: [10.1074/jbc.C113.543132](https://doi.org/10.1074/jbc.C113.543132)

Find articles, minireviews, Reflections and Classics on similar topics on the [JBC Affinity Sites](http://www.jbc.org/jbc/affinity).

Alerts:

- [When this article is cited](#)
- [When a correction for this article is posted](#)

[Click here](#) to choose from all of JBC's e-mail alerts

Supplemental material:

<http://www.jbc.org/jbc/suppl/2014/02/20/C113.543132.DC1.html>

This article cites 0 references, 0 of which can be accessed free at

<http://www.jbc.org/content/early/2014/02/20/jbc.C113.543132.full.html#ref-list-1>

Expression of a Synthetic 3-Hydroxypropionate Photorespiratory Bypass

Introduction of a Synthetic CO₂-Fixing Photorespiratory Bypass into a Cyanobacterium

Patrick M. Shih^{1,2}, Jan Zarzycki^{3,4}, Krishna K. Niyogi^{*1,2,4}, Cheryl A. Kerfeld^{*1,3,4,5}

From the ¹Department of Plant and Microbial Biology, University of California, Berkeley, CA 94720.

²Howard Hughes Medical Institute, University of California, Berkeley, CA 94720. ³Department of Biochemistry and Molecular Biology, DOE Plant Research Laboratories, Michigan State University, East Lansing, MI 48824. ⁴Physical Biosciences Division, Lawrence Berkeley National Laboratory, Berkeley, CA 94720. ⁵Synthetic Biology Institute, University of California, Berkeley, CA 94720.

Running Title: *Expression of a Synthetic 3-Hydroxypropionate Photorespiratory Bypass*

*To whom correspondence may be addressed: Cheryl A. Kerfeld, Michigan State University, Plant Biology, 612 Wilson Road, East Lansing, MI 48824, (517) 432-4371, ckerfeld@lbl.gov. Or, Krishna K. Niyogi, 111 Koshland Hall, University of California, Berkeley, CA 94720, (510) 643-6602, niyogi@berkeley.edu.

Keywords: Photosynthesis, RuBisCO, Metabolic engineering, Bioenergy, Synthetic biology, Cyanobacteria, 3-hydroxypropionate bi-cycle, *Chloroflexus*, *Synechococcus*

Background: Photorespiration limits carbon fixation.

Results: Heterologous expression and functional activity of six enzymes from the 3-hydroxypropionate bi-cycle is demonstrated in cyanobacteria.

Conclusion: A synthetic CO₂-fixing photorespiratory bypass can be introduced into cyanobacteria.

Significance: The results lay the foundation for expressing an alternative CO₂ fixation pathway in cyanobacteria, algae, and plants.

ABSTRACT

Global photosynthetic productivity is limited by the enzymatic assimilation of CO₂ into organic carbon compounds. Ribulose-1,5-bisphosphate carboxylase/oxygenase (RuBisCO), the carboxylating enzyme of the Calvin-Benson (CB) cycle, poorly discriminates between CO₂ and O₂, leading to photorespiration and the loss of fixed carbon and nitrogen. With the advent of synthetic biology, it is now feasible to design, synthesize

and introduce biochemical pathways *in vivo*. We engineered a synthetic photorespiratory bypass based on the 3-hydroxypropionate bi-cycle into the model cyanobacterium, *Synechococcus elongatus* sp. PCC 7942. The heterologously expressed cycle is designed to function as both a photorespiratory bypass and an additional CO₂-fixing pathway, supplementing the CB cycle. We demonstrate the function of all six introduced enzymes and identify bottlenecks to be targeted in subsequent bioengineering. These results have implications for efforts to improve photosynthesis, and for the “green” production of high-value products of biotechnological interest.

Oxygenic photosynthesis is the primary source of nearly all biological energy. In this process, light is converted into chemical energy which is used to fix CO₂ in the CB cycle through the enzyme RuBisCO. The carboxylase activity of RuBisCO results in the addition of one molecule of CO₂ to one molecule of ribulose-1,5-bisphosphate to create two molecules of 3-

phosphoglycerate, thus fixing inorganic CO₂ into triose phosphates. However, the competing oxygenase activity of RuBisCO results in the loss of fixed carbon through a process termed photorespiration. One of the 'holy grails' of photosynthesis research has been to engineer RuBisCO to improve CO₂ fixation and reduce photorespiration; however, these attempts have been met with limited success. It has been shown that biochemical constraints as well as abiotic factors are crucial considerations in addressing the protein engineering of RuBisCO (1,2). Given this complexity, a more promising approach may be to accept the inherent 'flaws' of RuBisCO and improve net photosynthetic rates through engineered photorespiratory bypasses.

Photorespiration produces the toxic intermediate 2-phosphoglycolate, which is recycled through the photorespiratory C₂ cycle (Fig. 1A). This pathway is costly, requiring ATP and reducing equivalents in an elaborate reaction sequence involving more than a dozen enzymes and transporters. Furthermore, the reaction catalyzed by glycine decarboxylase, converting two glycine molecules into one serine in the C₂ cycle, releases both NH₃ and CO₂, resulting in a net loss of carbon and nitrogen. To date, only two studies have attempted to experimentally decrease the negative impacts of the photorespiratory C₂ cycle by expression of alternative glycolate metabolic pathways. Kebeish et al. (3) attempted to bypass most of the C₂ cycle by introducing the glycolate catabolic pathway from *E. coli* (4) into *Arabidopsis thaliana* chloroplasts. This pathway circumvents the loss of nitrogen, but the glyoxylate carboligase reaction results in the release of one CO₂ per two glyoxylate molecules (Fig. 1A). Although increased biomass was reported, interestingly, transformants expressing only the first enzyme of that pathway, glycolate dehydrogenase, showed similar results, rendering the approach controversial. In a second study, Maier et al. (5) introduced a glycolate oxidation cycle into *Arabidopsis* chloroplasts; however this pathway results in the release of even more CO₂ than the heterologously expressed glycolate catabolism pathway. In both cases, CO₂ release occurs in the chloroplast, where it can potentially be refixed by RuBisCO. The challenges associated with designing experimental approaches to mitigate the losses associated with

photorespiration are likewise underscored by results from systems-level genome-scale metabolic modeling that suggests photorespiration is essential for optimal photosynthesis (6).

Introduction of additional, synthetic CO₂ fixation pathways provide an approach to increasing photosynthesis, which circumvents the complexities associated with manipulating the C₂ cycle (7). Of the six known CO₂ fixation cycles in nature, only the 3-hydroxypropionate (3OHP) bi-cycle is completely oxygen insensitive (8,9), a key consideration when engineering pathways into oxygenic photoautotrophs. The 3OHP bi-cycle from the thermophilic anoxygenic phototroph *Chloroflexus aurantiacus* offers an attractive starting point for engineering efforts (10), because all of the necessary enzymes have been characterized (9). In this bi-cyclic pathway, bicarbonate is fixed by biotin-dependent acetyl-CoA carboxylase and propionyl-CoA carboxylase. The primary CO₂ fixation product resulting from the first cycle is glyoxylate, which is then fed into the second cycle, in which another bicarbonate is fixed and pyruvate is generated as the final product (9).

We designed a CO₂-fixing synthetic photorespiratory bypass based on the 3OHP bi-cycle (Fig. 1B). To experimentally validate the design, we introduced the requisite six genes, encoded in assembled DNA constructs spanning more than 16 kbp, to reassimilate the photorespiratory byproduct glyoxylate in the cyanobacterium *S. elongatus* PCC7942. We demonstrate activity for all of the gene products and identify metabolic bottlenecks to be addressed. In comparison to the conventional C₂ cycle, the synthetic bypass not only prevents the loss of NH₃ but also results in a net gain in carbon fixation rather than a net loss.

EXPERIMENTAL PROCEDURES

Cloning, strains and growth conditions – All constructs were cloned using the BglBrick assembly format (11) in *E. coli* and subsequently cloned into various neutral site destination vectors, which allow for genomic integration into the *S. elongatus* genome by previously described transformation protocols (12,13). Plasmids and strains that were generated and used are summarized in Tables 1. All used primers are listed in Supplemental Table S1..

S. elongatus strains were maintained in BG-11 medium under appropriate selection with constant light at 30 or 37°C.

Cloning, heterologous expression of recombinant enzymes in E. coli, and purification - The cloning, expression, and purification of the mesaconyl-C1-CoA hydratase (MCH) and mesaconyl-CoA C1:C4 CoA transferase (MCT) from *C. aurantiacus* was performed as previously described (9). Cloning, expression, and purification of the malyl-CoA lyase (MCL) from *C. aurantiacus* was described previously (14). For the expression and purification of the MCT from '*Candidatus* Accumulibacter phosphatis' see Supplemental Data.

Enzyme assays - One unit (U) corresponds to an enzyme activity of 1 $\mu\text{mol min}^{-1}$ (mg protein^{-1}). Unless stated otherwise all assays were carried out at 30 or 37 °C, depending on the growth conditions of the transformant cultures. Cells were harvested during exponential phase by centrifugation at 6000 $\times g$. Cell pellets were resuspended in a two-fold volume of 200 mM MOPS/KOH buffer (pH 7.5). The cell suspensions were sonicated and the cell lysates were centrifuged at 20,000 $\times g$ and 4°C for 30 min. Supernatants were either used directly for enzyme assays or stored at -80°C.

The malonyl-CoA reductase was measured by a slightly modified previously described assay (15) monitoring the malonyl-CoA dependent oxidation of NADPH at a wavelength of 365 nm ($\epsilon_{365} = 3,400 \text{ M}^{-1} \text{ cm}^{-1}$). The assay mixture (400 μl) contained 200 mM MOPS/KOH buffer (pH 7.5), 5 mM MgCl_2 , 0.4 mM NADPH, and cell extract. The reaction was started by addition of 1 mM malonyl-CoA. Notably, two NADPH molecules are oxidized per one malonyl-CoA that is reduced to 3OHP.

Propionyl-CoA synthase activity was either monitored by a previously described and slightly modified spectrophotometric assay (16) or in an HPLC-based assay. (i) The reaction mixture (400 μl) for the photometric assay contained 200 mM MOPS/KOH buffer (pH 7.5), 0.4 mM NADPH, 100 mM KCl, 2 mM ATP, 0.5 mM CoA, and cell extract. The reaction was started by addition of 5 mM 3OHP. (ii) The same reaction mixture was used for the HPLC-based assay only with 1 mM instead of 0.4 mM NADPH. Samples of 100 μl were withdrawn after different time points and

stopped by addition of 10 μl 90% formic acid. The samples were kept on ice before precipitated protein was removed by centrifugation at 16,000 $\times g$. The supernatants were subjected to HPLC analysis to confirm propionyl-CoA formation.

The concerted function of the MCL, MCH, MCT, and mesaconyl-C4-CoA hydratase (MEH) was demonstrated in an HPLC-based assay. The reaction mixture (400 μl) contained 200 mM MOPS/KOH buffer (pH 7.5), 5 mM MgCl_2 , 0.5 mM propionyl-CoA, and cell extract. The reaction was started by addition of 5 mM glyoxylate and carried out at 37 °C. Samples of 100 μl were withdrawn after different time points and treated as described above and subjected to HPLC analysis to confirm the formation of acetyl-CoA or other CoA-thioester intermediates.

MCT activity was determined in a high performance liquid chromatography (HPLC)-based assay. The reaction mixture (0.4 ml) containing 200 mM MOPS/KOH (pH 7.5), 5 mM MgCl_2 , 2 mM propionyl-CoA, 10 mM glyoxylate, 3 U (formation of β -methylmalyl-CoA) of recombinant MCL, and 25 U of recombinant MCH was preincubated for 10 min at 37° C to form mesaconyl-C1-CoA as substrate for the CoA transferase. MCT or ApMCT was added to start the reaction. 100 μl samples were withdrawn prior to and after MCT addition. Reactions were stopped by addition of 5 μl of 90% formic acid. Precipitated protein was removed by centrifugation, and the supernatants were analyzed for CoA thioesters by reversed-phase HPLC. To determine the K_m value for mesaconyl-C1-CoA, a similar preincubation (0.2 ml) with 3 U of MCL and 25 U of MCH was performed for 15 min at 55°C with 10 mM propionyl-CoA and 30 mM glyoxylate. The reaction was stopped by addition of 2 μl of 90% formic acid. Precipitated protein was removed by centrifugation and the enzymatically synthesized mesaconyl-C1-CoA was used in the MCT assay at varying final concentrations as determined by HPLC and absorption at 260 nm.

Other methods – See Supplemental Data.

RESULTS

To implement the proposed cycle shown in Figure 1B, we first tested the constitutive expression and activity of the first four *Chloroflexus* enzymes required, beginning where

glyoxylate enters the cycle (*i.e.* MCL, MCH, MCT, and MEH). The reactions catalyzed by this sequence of enzymes result in the formation of acetyl-CoA and pyruvate (Fig. 1B) from propionyl-CoA and glyoxylate. Dicistronic operons were assembled to express *mcl* with *mch* and *mct* together with *meh* (Fig. 2A). Both dicistrons were driven by the previously characterized *psbAI* promoter (17). The cassette expressing all four genes (referred to as PMS4032) was integrated into the *S. elongatus* genome at Neutral Site 1 (NS1) (18). The resulting transformants were assayed for activity of all four enzymes. Soluble cell extracts from the transformants were incubated with propionyl-CoA and glyoxylate, and the expected disproportionation into acetyl-CoA and pyruvate was confirmed, indicating activity of all four enzymes; the rate of catalysis, however, was low.

The intermediates involved in the last two steps needed to complete the pathway in *S. elongatus*, MCR and PCS, are toxic to cells. Accumulation of 3OHP, the product of MCR, can lead to organic acid toxicity (19); propionyl-CoA, the product of PCS inhibits both pyruvate dehydrogenase and citrate synthase (20). The potential toxicity in conjunction with the difficulty of successfully reconstituting multi-step metabolic pathways (21) presented major challenges. Moreover, both MCR and PCS are large multi-domain enzymes, potentially presenting difficulty in proper folding and expression. For these reasons, *mcr* and *pcs* were driven by the IPTG-inducible promoter, pTrc (Fig. 2A). The *mcr* gene was assembled upstream of the PMS4032 cassette to generate PMS4570 and integrated into NS1 without an additional terminator downstream of *mcr*, whereas *pcs* alone was inserted into Neutral Site 3 (NS3) (13). Double transformants (PCS/PMS4570) containing all six genes integrated into both NS1 and NS3, were generated and tested for expression and enzyme activity in response to varying IPTG concentrations. MCR activity was confirmed spectrophotometrically by measuring the malonyl-CoA dependent oxidation of NADPH. PCS activity was measured by spectrophotometrically, by monitoring the 3OHP-dependent oxidation of NADPH and by following the formation of propionyl-CoA by HPLC. Both MCR and PCS were copiously expressed (Fig. 2B) and found to be active in the cell extracts (Fig. 2C

and 2D, respectively). An IPTG concentration of 20 μ M yielded the highest enzyme activities; further increases in IPTG concentrations did not result in higher activities. Furthermore, the addition of the pTrc promoter upstream of *mcr* also increased the expression of the two downstream genes *mcl* and *mch*, as deduced from the results of enzyme activity assays. However, the conversion of propionyl-CoA and glyoxylate to acetyl-CoA and pyruvate was stalled at the mesaconyl-C1-CoA intermediate (see Fig. 1). Addition of purified recombinant MCT to the assay resulted in immediate conversion of mesaconyl-C1-CoA to acetyl-CoA and pyruvate, indicating that *mct* expression was the bottleneck, whereas the *meh* gene downstream of *mct* was adequately expressed (Fig. 2E).

To relieve the bottleneck, a second copy of *mct*, driven by the IPTG-inducible pTrc promoter, was added upstream of *mcr*. We tested two strategies for introducing the additional *mct* gene: 1) adding a duplicate *Chloroflexus mct* to generate PMS4749 and 2) introducing a synthetic *mct* homolog (referred to as ApMCT) from the β -proteobacterium '*Candidatus* Accumulibacter phosphatis' (22,23) resulting in PMS4591 (Fig. 2A). ApMCT is the most closely related mesophilic homolog to the *Chloroflexus* MCT (24). We confirmed its function by expressing in *E. coli* and purifying a recombinant His₁₀-tagged version of the ApMCT, which catalyzed the expected intramolecular CoA transfer reaction within mesaconyl-CoA with a specific activity of $37 \pm 6 \mu\text{mol min}^{-1} (\text{mg protein})^{-1}$ at 37°C, corresponding to a turnover number (k_{cat}) of 58 s^{-1} per dimer. Its apparent K_m value for mesaconyl-C1-CoA was determined to be $1.49 \pm 0.22 \text{ mM}$, which was surprisingly high. In comparison the K_m value of the *Chloroflexus* MCT is only 0.24 mM (9). Moreover, the specific activity of the *Chloroflexus* MCT is much higher, $520 \mu\text{mol min}^{-1} (\text{mg protein})^{-1}$ at 55°C (9), even assuming the reaction would be halved each 10°C the temperature is decreased. Therefore, the overall efficiency of the ApMCT would be much lower.

Nevertheless, the double transformants encoding either a second *mct* gene from *Chloroflexus* or the *Accumulibacter* gene (PCS/PMS4749 or PCS/PMS4591, respectively) were generated (Fig. 2A) and assayed for all enzyme activities. In both cases the MCT activity

was substantially increased, and the activity of all six enzymes engineered into *S. elongatus* was confirmed (Fig. 2C, 2D, 2E, & 2G). However, introduction of the additional *mct* gene upstream of *mcr* apparently led to a decrease in MCR, MCL and MCH expression (Fig. 2B) and activity (Fig. 2F).

In order to estimate if the resulting enzyme activities were high enough to allow the functioning of the synthetic photorespiratory bypass, we calculated the carbon assimilation rate of a *S. elongatus* wild-type culture using the equation $dS/dt = (\mu/Y) \times X$ (25), which correlates the specific substrate consumption (dS) over time (dt) with the specific growth rate (μ). The established growth yield (Y) corresponds to a bacterial cell dry mass of 1 g formed per 0.5 g of carbon fixed (approx. 50% of bacterial cell dry mass is carbon). Although X usually refers to the concentration of living cells, in this case it is used to account for the amount of total protein per 1 g cell dry mass (in bacteria approx. 50% of cell dry mass is protein). We assumed a typical doubling time of 8 h for a wild-type culture under laboratory conditions with ambient CO_2 , which corresponds to a μ of 0.087 h^{-1} . This would require a net carbon assimilation rate of $121\text{ nmol min}^{-1}(\text{mg protein})^{-1}$. Taking into account an estimated loss of up to 25% of the fixed carbon due to photorespiration (26) results in $80\text{ nmol min}^{-1}(\text{mg protein})^{-1}$ for the oxygenase activity of RuBisCO and the production of glycolate. To efficiently reassimilate glycolate in the synthetic bypass the minimal specific activities of the involved enzymes need to be at least as high as the rate of glycolate generation. Based on that estimate all but one of the introduced enzymes were well above the required threshold (Figure 2G). Only the specific activity of PCS ($\sim 25\text{ nmol min}^{-1}(\text{mg protein})^{-1}$) in the transformant cell extracts was lower than the calculated threshold, despite very high expression (Fig. 2B).

DISCUSSION

This study is, to our knowledge, the first successful effort to express a synthetic CO_2 -fixing photorespiratory bypass in a photoautotrophic organism, the cyanobacterium *S. elongatus* PCC7942. Unlike previous studies, our pathway differs by directly avoiding the net loss of nitrogen and carbon in the photorespiratory C_2 cycle, which

actually results in a net gain in carbon fixation through the enzyme acetyl-CoA carboxylase (ACC).

The unique feature of our pathway is the additional carbon fixation, which must be accounted for in energy balance comparisons to other proposed photorespiratory bypasses. Therefore we have assumed the stoichiometrically correct values for the formation of two glycolate molecules per CO_2 released in the C_2 cycle (see Table 2). Thus, to reassimilate two glycolate molecules our cyclic bypass requires 6 ATP equivalents and 4 NAD(P)H, while fixing two additional molecules of bicarbonate, the form of inorganic carbon concentrated in the cytoplasm of cyanobacteria, and circumventing the loss of NH_3 . Note that if pyruvate, which derives from our bypass, is to be used for replenishing the CB cycle two more ATP equivalents are required per pyruvate molecule in gluconeogenesis by pyruvate phosphate dikinase, because it is AMP-forming. Nevertheless, the synthetic bypass compares favorably over the canonical photorespiratory C_2 cycle of cyanobacteria in terms of energy demand: the combined function of the C_2 cycle and CB cycle requires 11 ATP equivalents, 4 NAD(P)H, and 2 reduced ferredoxins to first refix the lost CO_2 and NH_3 , as well as additionally fix two more CO_2 molecules to arrive at the same level of net carbon fixation as the synthetic bypass (see Figure 1 and Table 2 for comparison of photorespiratory pathways).

Whereas the vast majority of metabolic engineering efforts focus on introducing linear pathways for the anabolic production of molecules of interest, our approach introduces a self-sustaining metabolic cycle that fixes CO_2 when glycolate/glyoxylate is available.

We demonstrate that concomitant expression and activity of all six enzymes necessary to reconstitute the synthetic bypass can be achieved. This required heterologous expression of ~ 16 kbp of DNA and functional assembly of six multimeric enzymes ranging in molecular mass from 62-600 kDa.

However, an obvious physiological phenotype was not observed during growth experiments. The transformants exhibited only slight delay in growth when liquid cultures in air were inoculated from agar plates, but they reached the same doubling times and optical densities as the wild

type (Figure 2F). Our results immediately suggest next steps toward improvement. For example, our initial design used enzymes derived from the thermophile *Chloroflexus* which are evolved to function at higher temperatures than the mesophilic growth conditions of plants and most cyanobacteria. This may underlie the low measured activity of heterologous PCS despite its strong overexpression in our transformants (Fig. 2B). Synthesis and assembly of such a large enzyme (~600 kDa) might impose a considerable stress on the transformant strains. Substitution by a PCS homolog from a mesophile may improve assembly and function of this trimeric enzyme in *S. elongatus*. Mining genome databases for mesophilic homologs of the six enzymes that may exhibit faster enzyme kinetics at lower temperatures could greatly improve flux through the cycle. However, characterization of these mesophilic alternatives is necessary, as our results with the much less efficient ApMCT homolog demonstrate. Nevertheless, mesophilic enzymes may still be advantageous in terms of expression and correct folding at ambient temperatures.

Likewise, an increase in ACCase activity may be required. Our present design relies on the native enzyme to fix bicarbonate. ACCase is required for fatty acid biosynthesis and endogenous levels of the enzyme may be insufficient to support optimal flux through the heterologously expressed cycle. However, overexpression of up to four separate subunits of the prokaryotic ACCases will significantly complicate DNA assembly and cloning strategies. Suitable alternatives may be eukaryotic ACCases, which have undergone gene fusion events creating one large single multi-functional gene (27).

In addition to the C₂ cycle, cyanobacteria can make use of two other strategies, the decarboxylation and glycerate pathways (28,29,30) that consume glyoxylate; they potentially compete with the synthetic bypass for substrate. In contrast, plants contain only the C₂ cycle, thus simplifying the fate of glyoxylate. With the localization of all six genes of our pathway to the chloroplast, only one additional enzyme, glycolate dehydrogenase, would be necessary to convert glyoxylate and bicarbonate to pyruvate. In fact, glycolate dehydrogenase has already been successfully targeted and expressed in chloroplasts of *Arabidopsis* (3).

Our results have implications beyond the optimization of photorespiration in plants and cyanobacteria. The successful introduction of half of the 3OHP bi-cycle into *S. elongatus* provides a platform in which to express the other half to attain the full bi-cyclic CO₂ fixation pathway. Given that CO₂ fixation limits the light-saturated rate of photosynthesis, the presence of two orthogonal CO₂ fixation pathways is expected to significantly enhance the conversion of solar energy into biomass. Although appealing, introducing the whole 3OHP bi-cycle will result in substantial carbon flux towards pyruvate, which could be detrimental to organisms that have evolved carbon metabolism based on sugar phosphates.

On the other hand, pyruvate or intermediates in the synthetic bypass could be redirected for biotechnological applications, such as biofuels or replacements for chemical feedstocks that are currently petroleum-derived (19). For example, we have shown that 3OHP, a precursor for bioplastics, can be derived from malonyl-CoA by the heterologous expression of MCR in cyanobacteria. Developing cyanobacteria as production strains requires increasing their tolerance to higher concentrations of 3OHP; this has been accomplished in *E. coli* (19). Likewise the production of propionyl-CoA by the combined function of MCR and PCS in the synthetic bypass could be useful for the production of diverse polyhydroxyalkanoates like polyhydroxyvalerate, polyhydroxymethylvalerate or co-polymers.

It is generally assumed that an increase in carbon fixation or decrease in photorespiration will improve the efficiency of photosynthesis (7) and thereby increase growth rates or biomass production; however, the effects on such broad and complex physiological traits are determined by many additional factors (e.g. carbon allocation, translocation, and secretion). Although our growth phenotype is inconclusive (Fig. 2F), future efforts in improving the properties (e.g. finding mesophilic homologs) of the enzymes used in our pathway will be crucial to further investigate the physiological impacts of synthetic carbon fixation pathways and photorespiratory bypasses. However, although several strategies dealing with photorespiration are known to exist in cyanobacteria its importance is not quite clear, especially in light of the cyanobacterial carbon

concentrating mechanisms that include the carboxysome. Moreover, we still do not fully understand all the effects of the introduced enzymes *in vivo*, thus future efforts relying on global and systems approaches may shed light on potential avenues for pathway optimization, as utilized in *E. coli* metabolic engineering efforts (31,32). This study represents an advance towards understanding the effects of altering central carbon metabolism in photosynthetic autotrophs using

synthetic biology and metabolic engineering approaches.

In summary, improving photosynthesis holds promise for increasing the sustainable production of food and biofuel crops to meet the challenges of global climate change and population growth, but introducing new pathways and cycles constitutes a daunting challenge. The synthetic photorespiratory bypass reported in this study provides both a precedent and a platform for future bioengineering efforts.

REFERENCES

1. Savir, Y., Noor, E., Milo, R., and Tlustý, T. (2010) Cross-species analysis traces adaptation of Rubisco toward optimality in a low-dimensional landscape. *Proc. Natl. Acad. Sci. U. S. A.* **107**, 3475-3480
2. Tcherkez, G. G., Farquhar, G. D., and Andrews, T. J. (2006) Despite slow catalysis and confused substrate specificity, all ribulose biphosphate carboxylases may be nearly perfectly optimized. *Proc. Natl. Acad. Sci. U. S. A.* **103**, 7246-7251
3. Kebeish, R., Niessen, M., Thiruveedhi, K., Bari, R., Hirsch, H. J., Rosenkranz, R., Stabler, N., Schonfeld, B., Kreuzaler, F., and Peterhansel, C. (2007) Chloroplastic photorespiratory bypass increases photosynthesis and biomass production in *Arabidopsis thaliana*. *Nat. Biotechnol.* **25**, 593-599
4. Pellicer, M. T., Badia, J., Aguilar, J., and Baldomà, L. (1996) *glc* locus of *Escherichia coli*: characterization of genes encoding the subunits of glycolate oxidase and the *glc* regulator protein. *J. Bacteriol.* **178**, 2051-2059
5. Maier, A., Fahnenstich, H., Von Caemmerer, S., Engqvist, M. K. M., Weber, A. P. M., Flügge, U.-I., and Maurino, V. G. (2012) Glycolate oxidation in *A. thaliana* chloroplasts improves biomass production. *Front Plant Sci* **3**, 38
6. Nogales, J., Gudmundsson, S., Knight, E. M., Palsson, B. O., and Thiele, I. (2012) Detailing the optimality of photosynthesis in cyanobacteria through systems biology analysis. *Proc Natl Acad Sci* **109**, 2678-2683
7. Blankenship, R. E., Tiede, D. M., Barber, J., Brudvig, G. W., Fleming, G., Ghirardi, M., Gunner, M. R., Junge, W., Kramer, D. M., Melis, A., Moore, T. A., Moser, C. C., Nocera, D. G., Nozik, A. J., Ort, D. R., Parson, W. W., Prince, R. C., and Sayre, R. T. (2011) Comparing photosynthetic and photovoltaic efficiencies and recognizing the potential for improvement. *Science* **332**, 805-809
8. Fuchs, G. (2011) Alternative pathways of carbon dioxide fixation: Insights into the early evolution of life? *Annu. Rev. Microbiol.* **65**, 631-658
9. Zarzycki, J., Brecht, V., Müller, M., and Fuchs, G. (2009) Identifying the missing steps of the autotrophic 3-hydroxypropionate CO₂ fixation cycle in *Chloroflexus aurantiacus*. *Proc Natl Acad Sci* **106**, 21317-21322
10. Mattozzi, M., Ziesack, M., Voges, M. J., Silver, P. A., and Way, J. C. (2013) Expression of the sub-pathways of the *Chloroflexus aurantiacus* 3-hydroxypropionate carbon fixation bicycle in *E. coli*: Toward horizontal transfer of autotrophic growth. *Metab Eng* **16**, 130-139
11. Anderson, J. C., Dueber, J., Leguia, M., Wu, G., Goler, J., Arkin, A., and Keasling, J. (2010) BglBricks: A flexible standard for biological part assembly. *J Biol Eng* **4**, 1

12. Mackey, S. R., Ditty, J. L., Clerico, E. M., and Golden, S. S. (2007) Detection of rhythmic bioluminescence from luciferase reporters in cyanobacteria. in *Circadian Rhythms* (Rosato, E. ed.), Humana Press. pp 115-129
13. Niederholtmeyer, H., Wolfstädter, B. T., Savage, D. F., Silver, P. A., and Way, J. C. (2010) Engineering cyanobacteria to synthesize and export hydrophilic products. *Appl. Environ. Microbiol.* **76**, 6023-6023
14. Zarzycki, J., and Kerfeld, C. A. (2013) The crystal structures of the tri-functional *Chloroflexus aurantiacus* and bi-functional *Rhodobacter sphaeroides* malyl-CoA lyases and comparison with CitE-like superfamily enzymes and malate synthases. *BMC Struct. Biol.* **13**, 28
15. Hügler, M., Menendez, C., Schägger, H., and Fuchs, G. (2002) Malonyl-coenzyme A reductase from *Chloroflexus aurantiacus*, a key enzyme of the 3-hydroxypropionate cycle for autotrophic CO₂ fixation. *J. Bacteriol.* **184**, 2404-2410
16. Alber, B. E., and Fuchs, G. (2002) Propionyl-Coenzyme A Synthase from *Chloroflexus aurantiacus*, a key enzyme of the 3-hydroxypropionate cycle for autotrophic CO₂ fixation. *J. Biol. Chem.* **277**, 12137-12143
17. Ducat, D. C., Sachdeva, G., and Silver, P. A. (2011) Rewiring hydrogenase-dependent redox circuits in cyanobacteria. *Proc Natl Acad Sci* **108**, 3941-3946
18. Clerico, E. M., Ditty, J. L., and Golden, S. S. (2007) Specialized techniques for site-directed mutagenesis in cyanobacteria. in *Circadian Rhythms* (Rosato, E. ed.), Humana Press. pp 155-171
19. Lipscomb, T. W., Lipscomb, M. L., Gill, R. T., and Lynch, M. D. (2012) Metabolic engineering of recombinant *E. coli* for the production of 3-hydroxypropionate. in *Engineering Complex Phenotypes in Industrial Strains*, John Wiley & Sons, Inc. pp 185-200
20. Horswill, A. R., Dudding, A. R., and Escalante-Semerena, J. C. (2001) Studies of propionate toxicity in *Salmonella enterica* identify 2-methylcitrate as a potent inhibitor of cell growth. *J. Biol. Chem.* **276**, 19094-19101
21. Keasling, J. D. (2010) Manufacturing molecules through metabolic engineering. *Science* **330**, 1355-1358
22. García Martín, H., Ivanova, N., Kunin, V., Warnecke, F., Barry, K. W., McHardy, A. C., Yeates, C., He, S., Salamov, A. A., Szeto, E., Dalin, E., Putnam, N. H., Shapiro, H. J., Pangilinan, J. L., Rigoutsos, I., Kyrpides, N. C., Blackall, L. L., McMahon, K. D., and Hugenholtz, P. (2006) Metagenomic analysis of two enhanced biological phosphorus removal (EBPR) sludge communities. *Nat. Biotechnol.* **24**, 1263-1269
23. Hesselmann, R. P., Werlen, C., Hahn, D., van der Meer, J. R., and Zehnder, A. J. (1999) Enrichment, phylogenetic analysis and detection of a bacterium that performs enhanced biological phosphate removal in activated sludge. *Syst. Appl. Microbiol.* **22**, 454-465
24. Zarzycki, J., and Fuchs, G. (2011) Coassimilation of organic substrates via the autotrophic 3-hydroxypropionate bi-cycle in *Chloroflexus aurantiacus*. *Appl. Environ. Microbiol.* **77**, 6181-6188
25. Hu, Z.-H., Yue, Z.-B., Liu, S.-Y., G.-P., S., and Yu, H.-Q. (2010) Anaerobic Digestion of Lignocellulosic Wastes by Rumen Microorganisms: Chemical and Kinetic Analyses. in *Environmental Anaerobic Technology: Applications and New Developments* (Fang, H. H. P. ed.), Imperial College Press, London. pp 259-278
26. Sharkey, T. D. (1988) Estimating the Rate of Photorespiration in Leaves. *Physiol. Plant* **73**, 147-152
27. Sasaki, Y., Konishi, T., and Nagano, Y. (1995) The Compartmentation of Acetyl-Coenzyme A Carboxylase in Plants. *Plant Physiol* **108**, 445-449
28. Eisenhut, M., Ruth, W., Haimovich, M., Bauwe, H., Kaplan, A., and Hagemann, M. (2008) The photorespiratory glycolate metabolism is essential for cyanobacteria and

- might have been conveyed endosymbiontically to plants. *Proc Natl Acad Sci* **105**, 17199-17204
29. Zarzycki, J., Axen, S. D., Kinney, J. N., and Kerfeld, C. A. (2013) Cyanobacterial-based approaches to improving photosynthesis in plants. *J. Exp. Bot.* **64**, 787-798
 30. Eisenhut, M., Kahlon, S., Hasse, D., Ewald, R., Lieman-Hurwitz, J., Ogawa, T., Ruth, W., Bauwe, H., Kaplan, A., and Hagemann, M. (2006) The plant-like C2 glycolate cycle and the bacterial-like glycerate pathway cooperate in phosphoglycolate metabolism in cyanobacteria. *Plant Physiol* **142**, 333-342
 31. Kizer, L., Pitera, D. J., Pfleger, B. F., and Keasling, J. D. (2008) Application of functional genomics to pathway optimization for increased isoprenoid production. *Appl. Environ. Microbiol.* **74**, 3229-3241.
 32. Dahl, R. H., Zhang, F., Alonso-Gutierrez, J., Baidoo, E., Batth, T. S., Redding-Johanson, A. M., Petzold, C. J., Mukhopadhyay, A., Lee, T.S., Adams, P. D., Keasling, J. D. (2013) Engineering dynamic pathway regulation using stress-response promoters. *Nat. Biotechnol.* **31**, 1039-1046.

ACKNOWLEDGMENTS

PMS was supported by NSF grant MCB0851054 to CAK and by the Gordon and Betty Moore Foundation grant GBMF3070 to KKN. JZ and CAK were also supported by the US DOE contract no. DE-AC02 05CH11231. KKN is an investigator of the Howard Hughes Medical Institute and the Gordon and Betty Moore Foundation. We thank Tim Hsiau, Josh Kittleson, and J. Chris Anderson's lab for sharing their expertise with DNA assembly strategies and technical assistance. We also thank David Savage for generously providing the pNS3 vector.

FIGURE LEGENDS

FIGURE 1. A) Schematic of the conventional photorespiratory C₂ cycle (red) in cyanobacteria and the glycerate bypass (turquoise), adapted from Zarzycki et al. (29). Reactions that take part in both pathways are colored purple. Ribulose-1,5-bisphosphate carboxylase/oxygenase (1), phosphoglycolate phosphatase (2), glycolate dehydrogenase (3), serine/glyoxylate aminotransferase (4), glutamate/glyoxylate aminotransferase (5), serine hydroxymethyltransferase (6), glycine decarboxylase (7), hydroxypyruvate reductase (8), glycerate kinase (9), glutamine synthetase (10), glutamine oxoglutarate aminotransferase (11), glyoxylate carboligase (12), tartronate-semialdehyde reductase (13). tetrahydrofolate (THF), methylenetetrahydrofolate (CH₂-THF), reduced ferredoxin (Fdx_{red}), oxidized ferredoxin (Fdx_{ox}). **B)** Engineering a synthetic cyclic photorespiratory bypass based on part of the 3OHP bi-cycle, which also fixes bicarbonate. Overview of the design and its intersection with the CB cycle. Enzymes in white boxes are present in cyanobacteria and plants. The six additional enzymes required to establish this CO₂ fixing photorespiratory bypass are in colored boxes. One bicarbonate molecule is fixed while one glyoxylate is consumed to form pyruvate, which can be used for biosynthesis or to replenish the CB cycle. Acc - acetyl-CoA carboxylase, Mcr - malonyl-CoA reductase; Pcs - propionyl-CoA synthase, Mcl - malyl-CoA lyase, Mch - mesaconyl-C1-CoA hydratase, Mct - mesaconyl-CoA C1:C4 CoA transferase, Meh - mesaconyl-C4-CoA hydratase, Pgp - 2-phosphoglycolate phosphatase, GlcD - glycolate dehydrogenase, RuBisCO - ribulose-1,5-bisphosphate carboxylase/oxygenase.

Figure 2. A) Schematic of assembled constructs and introduced genes integrated into the *S. elongatus* genome for generation of the PCS/PMS4570, PCS/PMS4591, and PCS/PMS4749 double transformants. Promoters and terminators are indicated by arrows and hairpins, respectively. Gene sizes and molecular weights of the functional enzymes are provided. Genes are colored as the corresponding enzymes in Fig. 1B. **B)** SDS-PAGE (coomassie stained) showing expression of the two large enzymes, MCR (malonyl-CoA reductase) and PCS (propionyl-CoA synthase). Lane 1 – mass standards, lanes 2-4 – cell extracts (25 µg protein each) of transformants PCS/PMS4570, PCS/PMS4591, PCS/PMS4749, respectively. **C)** Photometric assay for MCR activity monitoring the malonyl-CoA-dependent reduction of NADPH in transformant cell extract. **D)** Photometric assay for PCS activity monitoring the 3OHP-dependent reduction of NADPH in transformant cell extract. **E)** HPLC based assay demonstrating the disproportionation of glyoxylate and propionyl-CoA to pyruvate and acetyl-CoA by the coupled activity of MCL, MCH, MCT, and MEH in cell extracts of transformant PCS/PMS4749. **F)** Growth curve comparing the wild type to the two transformants with all introduced enzymes active. The transformants were grown in the presence of 20 µM IPTG from the beginning and the appropriate selection. **G)** Mean values (deviations <20%) were obtained from at least two independent measurements in cell extracts of replicate cultures. *Refers to the whole disproportionation of propionyl-CoA and glyoxylate to acetyl-CoA and pyruvate. §Reaction sequence stalls at mesaconyl-C1-CoA due to very low MCT activity.

Expression of a Synthetic 3-Hydroxypropionate Photorespiratory Bypass

TABLES

Table 1. List of plasmids/strains generated.

Construct	Host	Description	Insert Length	Reference
pAM1573	<i>S. elongatus</i>	Neutral Site 2 genomic integration vector		(12)
pAM1573PMS	<i>S. elongatus</i>	BglBrick modified pAM1573 vector		this work
pNS3	<i>S. elongatus</i>	Neutral site 3 genomic integration vector		(13)
pNS3:PCS	<i>S. elongatus</i>	pTrc:PCS	5492 bp	this work
PMS4032	<i>S. elongatus</i>	pPsbA1::rbs.mcl::rbs.mch::pPsbA1::rbs.mct::rbs.meh	5331 bp	this work
PMS4570	<i>S. elongatus</i>	pTrc::rbs.mcr::pPsbA1::rbs.mcl::rbs.mch::pPsbA1::rbs.mct::rbs.meh	9017 bp	this work
PMS4591	<i>S. elongatus</i>	pTrc::rbs.ApMct::rbs.mcr::pPsbA1::rbs.mcl::rbs.mch::pPsbA1::rbs.mct::rbs.meh	10244 bp	this work
PMS4749	<i>S. elongatus</i>	pTrc::rbs.mct::rbs.mcr::pPsbA1::rbs.mcl::rbs.mch::pPsbA1::rbs.mct::rbs.meh	10253 bp	this work
pET16b	<i>E. coli</i>	IPTG inducible expression vector		Novagen
pMct_Ap_JZ33	<i>E. coli</i>	IPTG inducible <i>Candidatus 'Accumulibacter phosphatis' mct</i>	855 bp	this work

Table 2: Energy balance comparison of photorespiratory pathways to achieve the same level carbon gain as the 3OHP bypass

	3OHP bypass (this study)	C ₂ (glycolate) cycle (30) + Calvin cycle	glycerate bypass (3) + Calvin cycle	glycolate oxidation (5) + Calvin Cycle
glycolate dehydrogenase (cyanobacteria)	+ 2 NAD(P)H	+ 2 NAD(P)H	+ 2 NAD(P)H	
glycine decarboxylase		+ 1 NADH - 1 CO ₂ - 1 NH ₃		
glutamine synthetase		- 1 ATP + NH ₃		
glutamine oxoglutarate aminotransferase		- 2 Fdx _(red)		
hydroxypyruvate reductase		- NADH		
glycerate kinase		- 1 ATP	- 1 ATP	
tartronic semialdehyde reductase			- 1 NADH	
glyoxylate carboligase			- 1 CO ₂	
malic enzyme				+ NADPH - 1 CO ₂
pyruvate dehydrogenase				+ NADH - 1 CO ₂
phosphoglycerate kinase		- 6 ATP	- 6 ATP	- 8 ATP
glyceraldehyde 3-phosphate dehydrogenase		- 6 NADPH	- 6 NADPH	- 8 NADPH
ribulose phosphate kinase		- 3 ATP	- 3 ATP	- 4 ATP
RubisCO		+ 3 CO ₂	+ 3 CO ₂	+ 4 CO ₂
acetyl-CoA carboxylase	- 2 ATP + 2 HCO ₃ ⁻			
malonyl-CoA reductase	- 4 NADPH			
propionyl-CoA synthase (AMP forming)	- 4 ATP equiv. - 2 NADPH			
pyruvate phosphate dikinase (AMP forming)*	- 4 ATP equiv.			
BALANCE	+ 2 HCO ₃ ⁻ - 6 ATP (- 10 ATP)* - 4 NAD(P)H	+ 2 CO ₂ - 11 ATP - 4 NAD(P)H - 2 Fdx _(red)	+ 2 CO ₂ - 10 ATP - 5 NAD(P)H	+ 2 CO ₂ - 12 ATP - 6 NAD(P)H

*If pyruvate is used for the regeneration of 3-phosphoglycerate 2 more ATP equivalents are required per pyruvate molecule by pyruvate phosphate dikinase (AMP-forming). Only 6 ATP are required if pyruvate is channeled into other biosyntheses pathways than gluconeogenesis.

FIGURES

Figure 1.

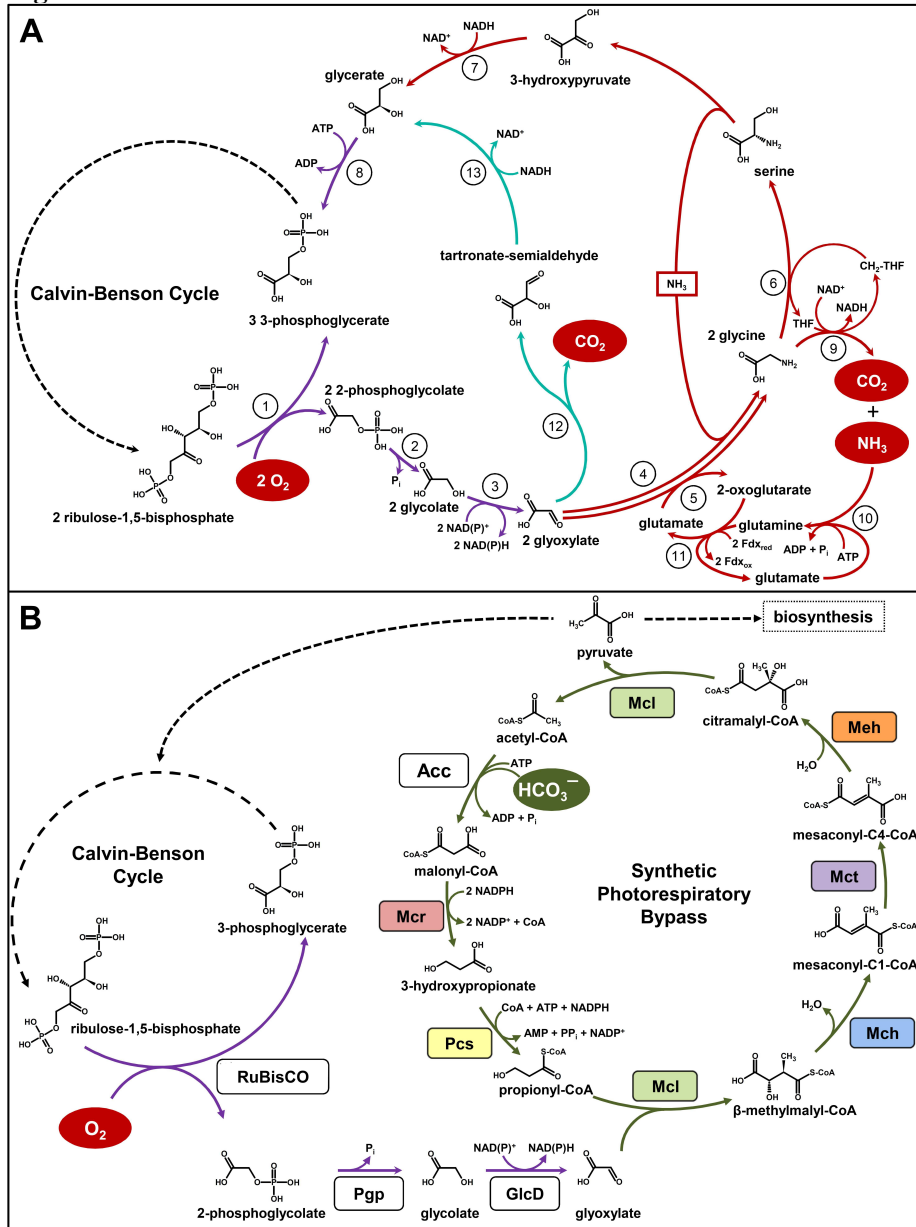


Figure 2.

